The standard model of particle physics

Mary K. Gaillard

University of California, Berkeley, California 94720

Paul D. Grannis

State University of New York, Stony Brook, New York 11794

Frank J. Sciulli

Columbia University, New York, New York 10027

Particle physics has evolved a coherent model that characterizes forces and particles at the most elementary level. This standard model, built from many theoretical and experimental studies, is in excellent accord with almost all current data. However, there are many hints that it is but an approximation to a yet more fundamental theory. The authors trace the development of the standard model and indicate the reasons for believing that it is incomplete. [S0034-6861(99)00202-0]

I. INTRODUCTION: A BIRD'S-EYE VIEW OF THE STANDARD MODEL

Over the past three decades a compelling case has emerged for the now widely accepted standard model of elementary particles and forces. A ''Standard Model'' is a theoretical framework built from observation that predicts and correlates new data. The Mendeleev table of elements was an early example in chemistry; from the periodic table one could predict the properties of many hitherto unstudied elements and compounds. Nonrelativistic quantum theory is another standard model that has correlated the results of countless experiments. Like its precursors in other fields, the standard model of particle physics has been enormously successful in predicting a wide range of phenomena. And, just as ordinary quantum mechanics fails in the relativistic limit, we do not expect the standard model to be valid at arbitrarily short distances. However, its remarkable success strongly suggests that the standard model will remain an excellent approximation to nature at distance scales as small as 10^{-18} m.

In the early 1960s particle physicists described nature in terms of four distinct forces, characterized by widely different ranges and strengths as measured at a typical energy scale of 1 GeV. The strong nuclear force has a range of about a fermi or 10^{-15} m. The weak force responsible for radioactive decay, with a range of 10^{-17} m, is about 10^{-5} times weaker at low energy. The electromagnetic force that governs much of macroscopic physics has infinite range and strength determined by the fine-structure constant, $\alpha \approx 10^{-2}$. The fourth force, gravity, also has infinite range and a low-energy coupling (about 10^{-38}) too weak to be observable in laboratory experiments. The achievement of the standard model was the elaboration of a unified description of the strong, weak, and electromagnetic forces in the language of quantum gauge-field theories. Moreover, the standard model combines the weak and electromagnetic forces in a single electroweak gauge theory, reminiscent of Maxwell's unification of the seemingly distinct forces of electricity and magnetism.

By midcentury, the electromagnetic force was well understood as a renormalizable quantum field theory (QFT) known as quantum electrodynamics or QED, described in the preceeding article. ''Renormalizable'' means that once a few parameters are determined by a limited set of measurements, the quantitative features of interactions among charged particles and photons can be calculated to arbitrary accuracy as a perturbative expansion in the fine-structure constant. QED has been tested over an energy range from 10^{-16} eV to tens of GeV, i.e., distances ranging from 10^{8} km to 10^{-2} fm. In contrast, the nuclear force was characterized by a coupling strength that precluded a perturbative expansion. Moreover, couplings involving higher spin states (resonances), which appeared to be on the same footing as nucleons and pions, could not be described by a renormalizable theory, nor could the weak interactions that were attributed to the direct coupling of four fermions to one another. In the ensuing years the search for renormalizable theories of strong and weak interactions, coupled with experimental discoveries and attempts to interpret available data, led to the formulation of the standard model, which has been experimentally verified to a high degree of accuracy over a broad range of energies and processes.

The standard model is characterized in part by the spectrum of elementary fields shown in Table I. The matter fields are fermions and their antiparticles, with half a unit of intrinsic angular momentum, or spin. There are three families of fermion fields that are identical in every attribute except their masses. The first family includes the up (u) and down (d) quarks that are the constituents of nucleons as well as pions and other mesons responsible for nuclear binding. It also contains the electron and the neutrino emitted with a positron in nuclear β decay. The quarks of the other families are constituents of heavier short-lived particles; they and

TABLE I. Elementary particles of the standard model: $S\hbar$ is spin, Qe is electric charge, and $m(\mathrm{GeV}/c^2)$ is mass. Numerical subscripts indicate the distinct color states of quarks and gluons.

Quarks: $S=\frac{1}{2}$				Leptons: $S=\frac{1}{2}$				Gauge bosons: $S=1$	
$Q=\frac{2}{3}$	m	$Q=-\frac{1}{3}$	m	$Q=-1$	m	$Q=0$	m	quanta	m
$u_1\ u_2\ u_3$	$(2-8)10^{-3}$	$d_1\ d_2\ d_3$	$(5-15)10^{-3}$	e	5.11×10^{-4}	ν_e	$<1.5\times10^{-8}$	$g_1\cdots g_8$	$<$ a few $\times10^{-3}$
$c_1\ c_2\ c_3$	1.0–1.6	$s_1\ s_2\ s_3$	0.1–0.3	μ	0.10566	ν_μ	$<1.7\times10^{-4}$	γ	$<6\times10^{-25}$
$t_1\ t_2\ t_3$	173.8 ± 5.0	$b_1\ b_2\ b_3$	4.1–4.5	τ	1.7770	ν_τ	$<1.8\times10^{-2}$	$W^{\pm},Z^0$	$80.39\pm0.06,91.187\pm0.002$

their companion charged leptons rapidly decay via the weak force to the quarks and leptons of the first family.

The spin-1 gauge bosons mediate interactions among fermions. In QED, interactions among electrically charged particles are due to the exchange of quanta of the electromagnetic field called photons (γ). The fact that the γ is massless accounts for the long range of the electromagnetic force. The strong force, quantum chromodynamics or QCD, is mediated by the exchange of massless gluons (g) between quarks that carry a quantum number called color. In contrast to the electrically neutral photon, gluons (the quanta of the "chromomagnetic" field) possess color charge and hence couple to one another. As a consequence, the color force between two colored particles increases in strength with increasing distance. Thus quarks and gluons cannot appear as free particles, but exist only inside composite particles, called hadrons, with no net color charge. Nucleons are composed of three quarks of different colors, resulting in "white" color-neutral states. Mesons contain quark and antiquark pairs whose color charges cancel. Since a gluon inside a nucleon cannot escape its boundaries, the nuclear force is mediated by color-neutral bound states, accounting for its short range, characterized by the Compton wavelength of the lightest of these: the π meson.

The even shorter range of the weak force is associated with the Compton wavelengths of the charged W and neutral Z bosons that mediate it. Their couplings to the "weak charges" of quarks and leptons are comparable in strength to the electromagnetic coupling. When the weak interaction is measured over distances much larger than its range, its effects are averaged over the measurement area and hence suppressed in amplitude by a factor $(E/M_{W,Z})^2\approx(E/100\ \mathrm{GeV})^2$, where E is the characteristic energy transfer in the measurement. Because the W particles carry electric charge they must couple to the γ, implying a gauge theory that unites the weak and electromagnetic interactions, similar to QCD in that the gauge particles are self-coupled. In distinction to γ's and gluons, W's couple only to left-handed fermions (with spin oriented opposite to the direction of motion).

The standard model is further characterized by a high degree of symmetry. For example, one cannot perform an experiment that would distinguish the color of the quarks involved. If the symmetries of the standard-model couplings were fully respected in nature, we would not distinguish an electron from a neutrino or a proton from a neutron; their detectable differences are attributed to "spontaneous" breaking of the symmetry. Just as the spherical symmetry of the earth is broken to a cylindrical symmetry by the earth's magnetic field, a field permeating all space, called the Higgs field, is invoked to explain the observation that the symmetries of the electroweak theory are broken to the residual gauge symmetry of QED. Particles that interact with the Higgs field cannot propagate at the speed of light, and acquire masses, in analogy to the index of refraction that slows a photon traversing matter. Particles that do not interact with the Higgs field—the photon, gluons, and possibly neutrinos—remain massless. Fermion couplings to the Higgs field not only determine their masses; they induce a misalignment of quark mass eigenstates with respect to the eigenstates of the weak charges, thereby allowing all fermions of heavy families to decay to lighter ones. These couplings provide the only mechanism within the standard model that can account for the observed violation of CP, that is, invariance of the laws of nature under mirror reflection (parity P) and the interchange of particles with their antiparticles (charge conjugation C).

The origin of the Higgs field has not yet been determined. However, our very understanding of the standard model implies that the physics associated with electroweak symmetry breaking must become manifest at energies of present-day colliders or at the LHC under construction. There is strong reason, stemming from the quantum instability of scalar masses, to believe that this physics will point to modifications of the theory. One shortcoming of the standard model is its failure to accommodate gravity, for which there is no renormalizable quantum field theory because the quantum of the gravitational field has two units of spin. Recent theoretical progress suggests that quantum gravity can be formulated only in terms of extended objects like strings and membranes, with dimensions of order of the Planck length 10^{-35} m. Experiments probing higher energies and shorter distances may reveal clues connecting the standard-model physics to gravity and may shed light on other questions that it leaves unanswered. In the following we trace the steps that led to the formulation of the standard model, describe the experiments that have confirmed it, and discuss some outstanding unresolved issues that suggest a more fundamental theory underlies the standard model.

II. THE PATH TO QCD

The invention of the bubble chamber permitted the observation of a rich spectroscopy of hadron states. At-

tempts at their classification using group theory, analogous to the introduction of isotopic spin as a classification scheme for nuclear states, culminated in the "Eightfold Way" based on the group SU(3), in which particles are ordered by their "flavor" quantum numbers: isotopic spin and strangeness. This scheme was spectacularly confirmed by the discovery at Brookhaven National Laboratory (BNL) of the Ω^- particle, with three units of strangeness, at the predicted mass. It was subsequently realized that the spectrum of the Eightfold Way could be understood if hadrons were composed of three types of quarks: u, d, and the strange quark s. However, the quark model presented a dilemma: each quark was attributed one-half unit of spin, but Fermi statistics precluded the existence of a state like the Ω^- composed of three strange quarks with total spin $\frac{3}{2}$. Three identical fermions with their spins aligned cannot exist in an an s-wave ground state. This paradox led to the hypothesis that quarks possess an additional quantum number called color, a conjecture supported by the observed rates for π^0 decay into $\gamma\gamma$ and e^+e^- annihilation into hadrons, both of which require three different quark types for each quark flavor.

A combination of experimental observations and theoretical analyses in the 1960s led to another important conclusion: pions behave like the Goldstone bosons of a spontaneously broken symmetry, called chiral symmetry. Massless fermions have a conserved quantum number called chirality, equal to their helicity: $+1$ for right-handed fermions and -1 for left-handed fermions. The analysis of pion scattering lengths and weak decays into pions strongly suggested that chiral symmetry is explicitly broken only by quark masses, which in turn implied that the underlying theory describing strong interactions among quarks must conserve quark helicity—just as QED conserves electron helicity. This further implied that interactions among quarks must be mediated by the exchange of spin-1 particles.

In the early 1970s, experimenters at the Stanford Linear Accelerator Center (SLAC) analyzed the distributions in energy and angle of electrons scattered from nuclear targets in inelastic collisions with momentum transfer $Q^2 \approx 1$ GeV/c from the electron to the struck nucleon. The distributions they observed suggested that electrons interact via photon exchange with pointlike objects called partons—electrically charged particles much smaller than nucleons. If the electrons were scattered by an extended object, e.g., a strongly interacting nucleon with its electric charge spread out by a cloud of pions, the cross section would drop rapidly for values of momentum transfer greater than the inverse radius of the charge distribution. Instead, the data showed a "scale-invariant" distribution: a cross section equal to the QED cross section up to a dimensionless function of kinematic variables, independent of the energy of the incident electron. Neutrino-scattering experiments at CERN and Fermilab (FNAL) yielded similar results. Comparison of electron and neutrino data allowed a determination of the average squared electric charge of the partons in the nucleon, and the result was consistent with the interpretation that they are fractionally charged quarks. Subsequent experiments at SLAC showed that, at center-of-mass energies above about two GeV, the final states in e^+e^- annihilation into hadrons have a two-jet configuration. The angular distribution of the jets with respect to the beam, which depends on the spin of the final-state particles, is similar to that of the muons in an $\mu^+\mu^-$ final state, providing direct evidence for spin-$\frac{1}{2}$ partonlike objects.

III. THE PATH TO THE ELECTROWEAK THEORY

A major breakthrough in deciphering the structure of weak interactions was the suggestion that they may not conserve parity, prompted by the observation of K decay into both 2π and 3π final states with opposite parity. An intensive search for parity violation in other decays culminated in the establishment of the "universal $V-A$ interaction." Weak processes such as nuclear β decay and muon decay arise from quartic couplings of fermions with negative chirality; thus only left-handed electrons and right-handed positrons are weakly coupled. Inverse β decay was observed in interactions induced by electron antineutrinos from reactor fluxes, and several years later the muon neutrino was demonstrated to be distinct from the electron neutrino at the BNL alternating-gradient synchrotron.

With the advent of the quark model, the predictions of the universal $V-A$ interaction could be summarized by introducing a weak-interaction Hamiltonian density of the form

$$H_w = \frac{G_F}{\sqrt{2}} J^\mu J^\dagger_\mu ,$$

$$J_\mu = \bar{d}\gamma_\mu(1-\gamma_5)u + \bar{e}\gamma_\mu(1-\gamma_5)\nu_e + \bar{\mu}\gamma_\mu(1-\gamma_5)\nu_\mu , \quad (1)$$

where G_F is the Fermi coupling constant, γ_μ is a Dirac matrix, and $\frac{1}{2}(1-\gamma_5)$ is the negative chirality projection operator. However, Eq. (1) does not take into account the observed β decays of strange particles. Moreover, increasingly precise measurements, together with an improved understanding of QED corrections, showed that the Fermi constant governing neutron β decay is a few percent less than the μ-decay constant. Both problems were resolved by the introduction of the Cabibbo angle θ_c and the replacement $d \to d_c = d\cos\theta_c + s\sin\theta_c$ in Eq. (1). Precision measurements made possible by high-energy beams of hyperons (the strange counterparts of nucleons) at CERN and FNAL have confirmed in detail the predictions of this theory with $\sin\theta_c \approx 0.2$.

While the weak interactions maximally violate P and C, CP is an exact symmetry of the Hamiltonian (1). The discovery at BNL in 1964 that CP is violated in neutral-kaon decay to two pions at a level of 0.1% in amplitude could not be incorporated into the theory in any obvious

way. Another difficulty arose from quantum effects induced by the Hamiltonian (1) that allow the annihilation of the antistrange quark and the down quark in a neutral kaon. This annihilation can produce a $\mu^+\mu^-$ pair, resulting in the decay $K^0\to\mu^+\mu^-$, or a $\bar{d}s$ pair, inducing K^0-$\bar{K}^0$ mixing. To suppress processes like these to a level consistent with experimental observation, a fourth quark flavor called charm (c) was proposed, with the current density in Eq. (1) modified to read

$$J_\mu=\bar{d}_c\gamma_\mu(1-\gamma_5)u+\bar{s}_c\gamma_\mu(1-\gamma_5)c + \bar{e}\gamma_\mu(1-\gamma_5)\nu_e+\bar{\mu}\gamma_\mu(1-\gamma_5)\nu_\mu,$$
$$s_c=s\cos\theta_c-d\sin\theta_c. \quad (2)$$

With this modification, contributions from virtual $c\bar{c}$ pairs cancel those from virtual $u\bar{u}$ pairs, up to effects dependent on the difference between the u and c masses. Comparison with experiment suggested that the charmed-quark mass should be no larger than a few GeV. The narrow resonance J/ψ with mass of about 3 GeV, found in 1974 at BNL and SLAC, was ultimately identified as a $c\bar{c}$ bound state.

IV. THE SEARCH FOR RENORMALIZABLE THEORIES

In the 1960s the only known renormalizable theories were QED and the Yukawa theory—the interaction of spin-$\frac{1}{2}$ fermions via the exchange of spinless particles. Both the chiral symmetry of the strong interactions and the $V-A$ nature of the weak interactions suggested that all forces except gravity are mediated by spin-1 particles, like the photon. QED is renormalizable because gauge invariance, which gives conservation of electric charge, also ensures the cancellation of quantum corrections that would otherwise result in infinitely large amplitudes. Gauge invariance implies a massless gauge particle and hence a long-range force. Moreover, the mediator of weak interactions must carry electric charge and thus couple to the photon, requiring its description within a Yang-Mills theory that is characterized by self-coupled gauge bosons.

The important theoretical breakthrough of the early 1970s was the proof that Yang-Mills theories are renormalizable, and that renormalizability remains intact if gauge symmetry is spontaneously broken, that is, if the Lagrangian is gauge invariant, but the vacuum state and spectrum of particles are not. An example is a ferromagnet for which the lowest-energy configuration has electron spins aligned; the direction of alignment spontaneously breaks the rotational invariance of the laws of physics. In quantum field theory, the simplest way to induce spontaneous symmetry breaking is the Higgs mechanism. A set of elementary scalars ϕ is introduced with a potential-energy density function $V(\phi)$ that is minimized at a value $\langle\phi\rangle\neq 0$ and the vacuum energy is degenerate. For example, the gauge-invariant potential for an electrically charged scalar field $\phi=|\phi|e^{i\theta}$,

$$V(|\phi|^2)=-\mu^2|\phi|^2+\lambda|\phi|^4, \quad (3)$$

has its minimum at $\sqrt{2}\langle|\phi|\rangle=\mu/\sqrt{\lambda}=v$, but is independent of the phase θ. Nature's choice for θ spontaneously breaks the gauge symmetry. Quantum excitations of $|\phi|$ about its vacuum value are massive Higgs scalars: $m_H^2=2\mu^2=2\lambda v^2$. Quantum excitations around the vacuum value of θ cost no energy and are massless, spinless particles called Goldstone bosons. They appear in the physical spectrum as the longitudinally polarized spin states of gauge bosons that acquire masses through their couplings to the Higgs field. A gauge-boson mass m is determined by its coupling g to the Higgs field and the vacuum value v. Since gauge couplings are universal this also determines the Fermi constant G for this toy model: $m=gv/2, G/\sqrt{2}=g^2/8m^2=v^2/2$.

The gauge theory of electroweak interactions entails four gauge bosons: $W^{\pm 0}$ of SU(2) or weak isospin $\vec{I}_w$, with coupling constant $g=e\sin\theta_w$, and B^0 of U(1) or weak hypercharge $Y_w=Q-I_w^3$, with coupling $g'=e\cos\theta_w$. Symmetry breaking can be achieved by the introduction of an isodoublet of complex scalar fields $\phi=(\phi^+\phi^0)$, with a potential identical to Eq. (3) where $|\phi|^2=|\phi^+|^2+|\phi^0|^2$. Minimization of the vacuum energy fixes $v=\sqrt{2}|\phi|=2^{1/4}G_F^{1/2}=246$ GeV, leaving three Goldstone bosons that are eaten by three massive vector bosons: $W^\pm$ and $Z=\cos\theta_w W^0-\sin\theta_w B^0$, while the photon $\gamma=\cos\theta_w B^0+\sin\theta_w W^0$ remains massless. This theory predicted neutrino-induced neutral-current interactions of the type $\nu+$ atom $\to\nu+$ anything, mediated by Z exchange. The weak mixing angle θ_w governs the dependence of the neutral-current couplings on fermion helicity and electric charge, and their interaction rates are determined by the Fermi constant G_F^Z. The ratio $\rho=G_F^Z/G_F=m_W^2/m_Z^2\cos^2\theta_w$, predicted to be 1, is the only measured parameter of the standard model that probes the symmetry-breaking mechanism. Once the value of θ_w was determined in neutrino experiments, the W and Z masses could be predicted: $m_W^2=m_Z^2\cos^2\theta_w=\sin^2\theta_w\pi\alpha/\sqrt{2}G_F$.

This model is not renormalizable with three quark flavors and four lepton flavors because gauge invariance is broken at the quantum level unless the sum of electric charges of all fermions vanishes. This is true for each family of fermions in Table I, and could be achieved by invoking the existence of the charmed quark, introduced in Eq. (2). However, the discovery of charmed mesons ($c\bar{u}$ and $c\bar{d}$ bound states) in 1976 was quickly followed by the discovery of the τ lepton, requiring a third full fermion family. A third family had in fact been anticipated by efforts to accommodate CP violation, which can arise from the misalignment between fermion gauge couplings and Higgs couplings provided there are more than two fermion families.

Meanwhile, to understand the observed scaling behavior in deep-inelastic scattering of leptons from nucleons, theorists were searching for an asymptotically free theory—a theory in which couplings become weak at short distance. The charge distribution of a strongly interacting particle is spread out by quantum effects, while scaling showed that at large momentum transfer quarks

behaved like noninteracting particles. This could be understood if the strong coupling becomes weak at short distances, in contrast to electric charge or Yukawa couplings that decrease with distance due to the screening effect of vacuum polarization. QCD, with gauged SU(3) color charge, became the prime candidate for the strong force when it was discovered that Yang-Mills theories are asymptotically free: the vacuum polarization from charged gauge bosons has the opposite sign from the fermion contribution and is dominant if there are sufficiently few fermion flavors. This qualitatively explains quark and gluon confinement: the force between color-charged particles grows with the distance between them, so they cannot be separated by a distance much larger than the size of a hadron. QCD interactions at short distance are characterized by weak coupling and can be calculated using perturbation theory as in QED; their effects contribute measurable deviations from scale invariance that depend logarithmically on the momentum transfer.

The standard model gauge group, $SU(3)\times SU(2)\times U(1)$, is characterized by three coupling constants $g_3=g_S$, $g_2=g$, $g_1=\sqrt{5/3}g'$, where g_1 is fixed by requiring the same normalization for all fermion currents. Their measured values at low energy satisfy $g_3>g_2>g_1$. Like g_3, the coupling g_2 decreases with increasing energy, but more slowly because there are fewer gauge bosons contributing. As in QED, the U(1) coupling increases with energy. Vacuum polarization effects calculated using the particle content of the standard model show that the three coupling constants are very nearly equal at an energy scale around 10^{16} GeV, providing a tantalizing hint of a more highly symmetric theory, embedding the standard-model interactions into a single force. Particle masses also depend on energy; the b and τ masses become equal at a similar scale, suggesting the possibility of quark and lepton unification as different charge states of a single field.

V. BRIEF SUMMARY OF THE STANDARD-MODEL ELEMENTS

The standard model contains the set of elementary particles shown in Table I. The forces operative in the particle domain are the strong (QCD) interaction, responsive to particles carrying color, and the two pieces of the electroweak interaction, responsive to particles carrying weak isospin and hypercharge. The quarks come in three experimentally indistinguishable colors and there are eight colored gluons. All quarks and leptons, as well as the γ, W, and Z bosons, carry weak isospin. In the strict view of the standard model, there are no right-handed neutrinos or left-handed antineutrinos. As a consequence the simple Higgs mechanism described in Sec. IV cannot generate neutrino masses, which are posited to be zero.

In addition, the standard model provides the quark mixing matrix which gives the transformation from the basis of the strong-interaction charge $-\frac{1}{3}$ left-handed quark flavors to the mixtures which couple to the electroweak current. The elements of this matrix are fundamental parameters of the standard model. A similar mixing may occur for the neutrino flavors, and if accompanied by nonzero neutrino mass, would induce weak-interaction flavor-changing phenomena that are outside the standard-model framework.

Finding the constituents of the standard model spanned the first century of the American Physical Society, starting with the discovery by Thomson of the electron in 1897. Pauli in 1930 postulated the existence of the neutrino as the agent of missing energy and angular momentum in β decay; only in 1953 was the neutrino found in experiments at reactors. The muon was unexpectedly added from cosmic-ray searches for the Yukawa particle in 1936; in 1962 its companion neutrino was found in the decays of the pion.

The Eightfold Way classification of the hadrons in 1961 suggested the possible existence of the three lightest quarks (u, d, and s), though their physical reality was then regarded as doubtful. The observation of substructure of the proton, the 1974 observation of the J/ψ meson interpreted as a $c\bar{c}$ bound state, and the observation of mesons with a single charm quark in 1976 cemented the reality of the first two generations of quarks. This state of affairs, with two symmetric generations of leptons and quarks, was theoretically tenable and the particle story very briefly seemed finished.

In 1976, the τ lepton was found in a SLAC experiment, breaking new ground into the third generation of fermions. The discovery of the Υ at FNAL in 1979 was interpreted as the bound state of a new bottom (b) quark. The neutrino associated with the τ has not been directly observed, but indirect measurements certify its existence beyond reasonable doubt. The final step was the discovery of the top (t) quark at FNAL in 1995. Despite the completed particle roster, there are fundamental questions remaining; chief among these is the tremendous disparity of the matter particle masses, ranging from the nearly massless neutrinos, the 0.5-MeV electron, and few-MeV u and d quarks, to the top quark whose mass is nearly 200 GeV. Even the taxonomy of particles hints at unresolved fundamental questions!

The gauge particle discoveries are also complete. The photon was inferred from the arguments of Planck, Einstein, and Compton early in this century. The carriers of the weak interaction, the W and Z bosons, were postulated to correct the lack of renormalizability of the four-Fermion interaction and given relatively precise predictions in the unified electroweak theory. The discovery of these in the CERN $p\bar{p}$ collider in 1983 was a dramatic confirmation of this theory. The gluon which mediates the color-force QCD was first demonstrated in the e^+e^- collider at DESY in Hamburg.

The minimal version of the standard model, with no right-handed neutrinos and the simplest possible electroweak symmetry-breaking mechanism, has 19 arbitrary parameters: nine fermion masses; three angles and one phase that specify the quark mixing matrix; three gauge coupling constants; two parameters to specify the Higgs potential; and an additional phase θ that charac-

terizes the QCD vacuum state. The number of parameters is larger if the electroweak symmetry-breaking mechanism is more complicated or if there are right-handed neutrinos. Aside from constraints imposed by renormalizability, the spectrum of elementary particles is also arbitrary. As will be discussed in Sec. VII, this high degree of arbitrariness suggests that a more fundamental theory underlies the standard model.

VI. EXPERIMENTAL ESTABLISHMENT OF THE STANDARD MODEL

The current picture of particles and interactions has been shaped and tested by three decades of experimental studies at laboratories around the world. We briefly summarize here some typical and landmark results.

A. Establishing QCD

1. Deep-inelastic scattering

Pioneering experiments at SLAC in the late 1960s directed high-energy electrons on proton and nuclear targets. The deep-inelastic scattering process results in a deflected electron and a hadronic recoil system from the initial baryon. The scattering occurs through the exchange of a photon coupled to the electric charges of the participants. Deep-inelastic scattering experiments were the spiritual descendents of Rutherford's scattering of α particles by gold atoms and, as with the earlier experiment, showed the existence of the target's substructure. Lorentz and gauge invariance restrict the matrix element representing the hadronic part of the interaction to two terms, each multiplied by phenomenological form factors or structure functions. These in principle depend on the two independent kinematic variables; the momentum transfer carried by the photon (Q^2) and energy loss by the electron (ν). The experiments showed that the structure functions were, to good approximations, independent of Q^2 for fixed values of $x = Q^2/2M\nu$. This "scaling" result was interpreted as evidence that the proton contains subelements, originally called partons. The deep-inelastic scattering occurs when a beam electron scatters with one of the partons. The original and subsequent experiments established that the struck partons carry the fractional electric charges and half-integer spins dictated by the quark model. Furthermore, the experiments demonstrated that three such partons (valence quarks) provide the nucleon with its quantum numbers. The variable x represents the fraction of the target nucleon's momentum carried by the struck parton, viewed in a Lorentz frame where the proton is relativistic. The deep-inelastic scattering experiments further showed that the charged partons (quarks) carry only about half of the proton momentum, giving indirect evidence for an electrically neutral partonic gluon.

Further deep-inelastic scattering investigations using electrons, muons, and neutrinos and a variety of targets

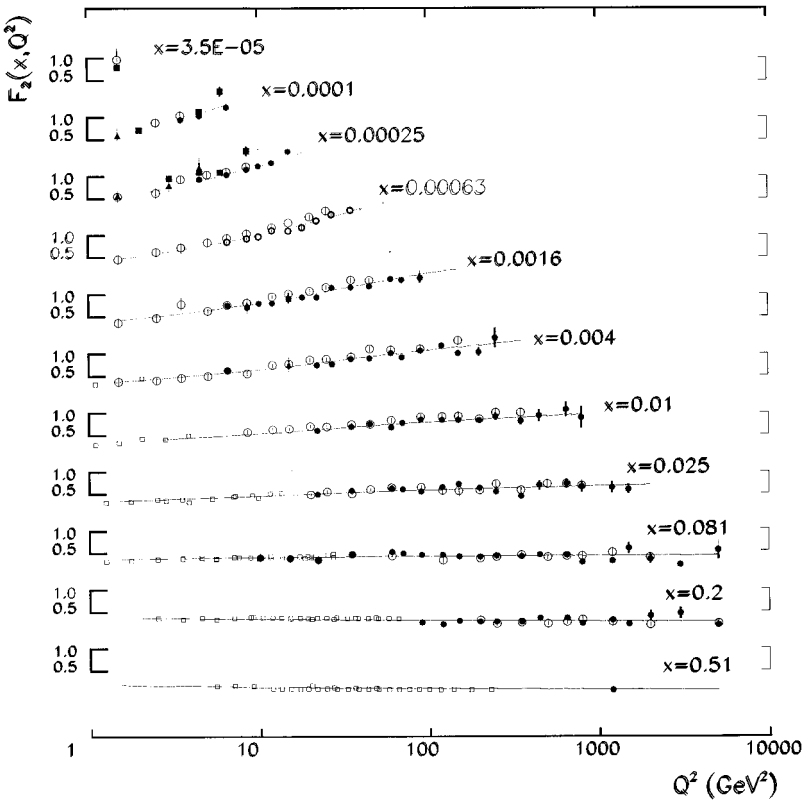

FIG. 1. The proton structure function F_2 vs Q^2 at fixed x, measured with incident electrons or muons, showing scale invariance at larger x and substantial dependence on Q^2 as x becomes small. The data are taken from the HERA ep collider experiments H1 and ZEUS, as well as the muon-scattering experiments BCDMS and NMC at CERN and E665 at FNAL.

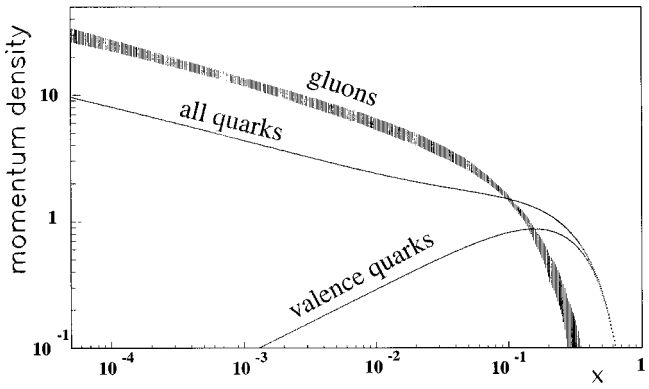

FIG. 2. The quark and gluon momentum densities in the proton vs x for $Q^2=20$ GeV^2. The integrated values of each component density give the fraction of the proton momentum carried by that component. The valence u and d quarks carry the quantum numbers of the proton. The large number of quarks at small x arises from a "sea" of quark-antiquark pairs. The quark densities are from a phenomenological fit (CTEQ collaboration) to data from many sources; the gluon density bands are the one-standard-deviation bounds to QCD fits to ZEUS data (low x) and muon-scattering data (higher x).

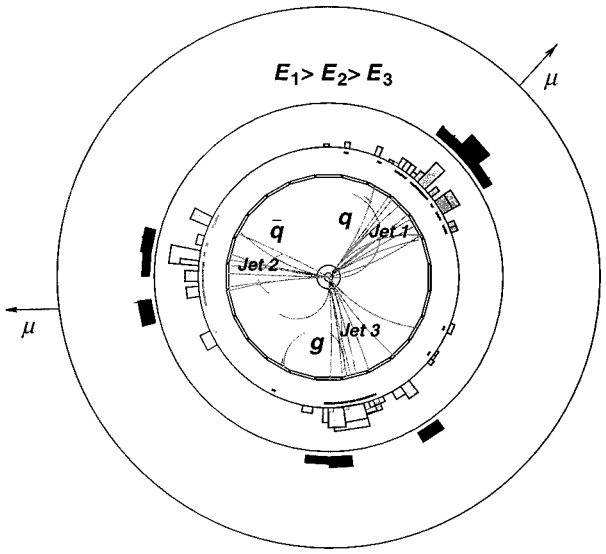

FIG. 3. A three-jet event from the OPAL experiment at LEP. The curving tracks from the three jets may be associated with the energy deposits in the surrounding calorimeter, shown here as histograms on the middle two circles, whose bin heights are proportional to energy. Jets 1 and 2 contain muons as indicated, suggesting that these are both quark jets (likely from b quarks). The lowest-energy jet 3 is attributed to a radiated gluon.

refined this picture and demonstrated small but systematic nonscaling behavior. The structure functions were shown to vary more rapidly with Q^2 as x decreases, in accord with the nascent QCD prediction that the fundamental strong-coupling constant α_S varies with Q^2 and that, at short distance scales (high Q^2), the number of observable partons increases due to increasingly resolved quantum fluctuations. Figure 1 shows sample modern results for the Q^2 dependence of the dominant structure-function, in excellent accord with QCD predictions. The structure-function *values* at all x depend on the quark content; the *increases* at larger Q^2 depend on both quark and gluon content. The data permit the mapping of the proton's quark and gluon content exemplified in Fig. 2.

2. Quark and gluon jets

The gluon was firmly predicted as the carrier of the color force. Though its presence had been inferred because only about half the proton momentum was found in charged constituents, direct observation of the gluon was essential. This came from experiments at the DESY e^+e^- collider (PETRA) in 1979. The collision forms an intermediate virtual photon state, which may subsequently decay into a pair of leptons or pair of quarks. The colored quarks cannot emerge intact from the collision region; instead they create many quark-antiquark pairs from the vacuum that arrange themselves into a set of colorless hadrons moving approximately in the directions of the original quarks. These sprays of roughly collinear particles, called jets, reflect the directions of the progenitor quarks. However, the quarks may radiate quanta of QCD (gluons) prior to formation of the jets, just as electrons radiate photons. If at sufficiently large angle to be distinguished, the gluon radiation evolves into a separate jet. Evidence for the "three-pronged" jet topologies expected for events containing a gluon was found in the event energy-flow patterns. Experiments at higher-energy e^+e^- colliders illustrate this gluon radiation even better, as shown in Fig. 3. Studies in e^+e^- and hadron collisions have verified the expected QCD structure of the quark-gluon couplings and their interference patterns.

3. Strong-coupling constant

The fundamental characteristic of QCD is asymptotic freedom, dictating that the coupling constant for color interactions decreases logarithmically as Q^2 increases. The coupling α_S can be measured in a variety of strong-interaction processes at different Q^2 scales. At low Q^2, deep-inelastic scattering, tau decays to hadrons, and the annihilation rate for e^+e^- into multihadron final states give accurate determinations of α_S. The decays of the Υ into three jets primarily involve gluons, and the rate for this decay gives $\alpha_S(M_\Upsilon^2)$. At higher Q^2, studies of the W and Z bosons (for example, the decay width of the Z, or the fraction of W bosons associated with jets) measure α_S at the 100-GeV scale. These and many other determinations have now solidified the experimental evidence that α_S does indeed "run" with Q^2 as expected in QCD. Predictions for $\alpha_S(Q^2)$, relative to its value at some reference scale, can be made within perturbative QCD. The current information from many sources is compared with calculated values in Fig. 4.

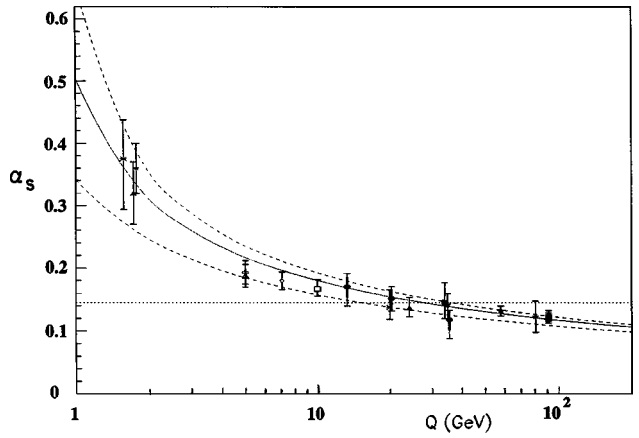

FIG. 4. The dependence of the strong-coupling constant α_S vs Q, using data from deep-inelastic-scattering structure functions from e, μ, and ν beam experiments as well as ep collider experiments, production rates of jets, heavy-quark flavors, photons, and weak vector bosons in ep, e^+e^-, and $p\bar{p}$ experiments. The data are in clear disagreement with a strong coupling independent of Q (horizontal line). All data agree with the dependence expected in QCD. The curves correspond to next-to-leading-order calculations of $\alpha_s(Q)$ evaluated using values for $\alpha_S(M_Z)$ of 0.1048, 0.1175, and 0.1240.

4. Strong-interaction scattering of partons

At sufficiently large Q^2 where α_S is small, the QCD perturbation series converges sufficiently rapidly to permit accurate predictions. An important process probing the highest accessible Q^2 scales is the scattering of two constituent partons (quarks or gluons) within colliding protons and antiprotons. Figure 5 shows the impressive data for the inclusive production of jets due to scattered partons in $p\bar{p}$ collisions at 1800 GeV. The QCD NLO predictions give agreement with the data over nine orders of magnitude in the cross section.

The angular distribution of the two highest-transverse-momentum jets from $p\bar{p}$ collisions reveals the

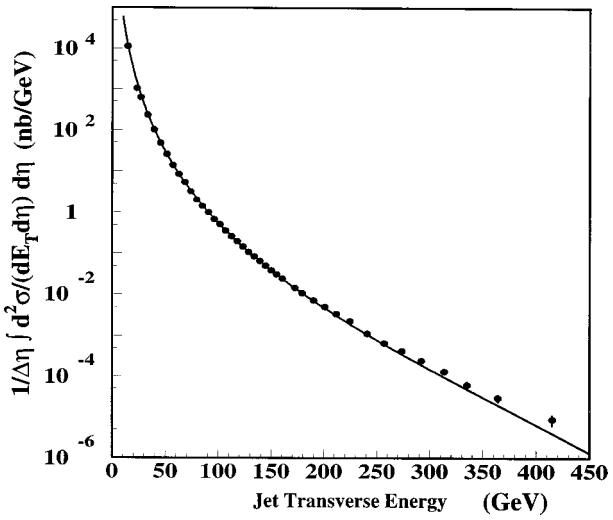

FIG. 5. Inclusive jet cross section vs jet transverse momentum. The data points are from the CDF experiment. The curve gives the prediction of next-to-leading-order QCD.

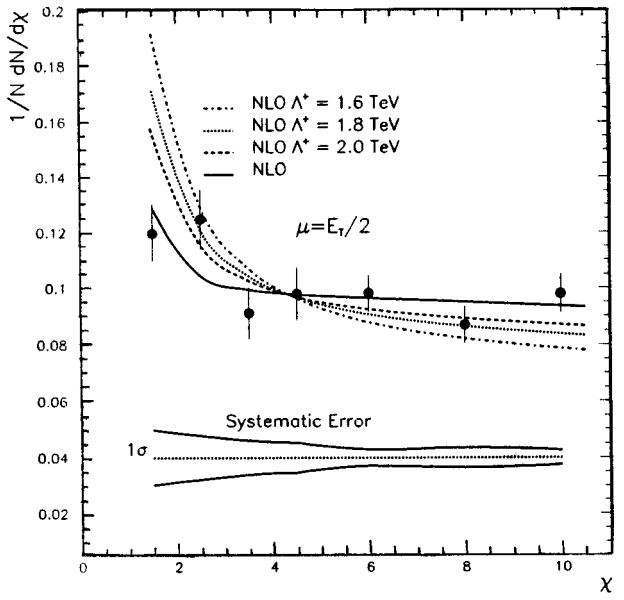

FIG. 6. The dijet angular distribution from the DØ experiment plotted as a function of χ (see text) for which Rutherford scattering would give $d\sigma/d\chi=$constant. The predictions of next-to-leading-order QCD (at scale $\mu=E_T/2$) are shown by the curves. Λ is the compositeness scale for quark/gluon substructure, with $\Lambda=\infty$ for no compositness (solid curve); the data rule out values of $\Lambda<2$ TeV.

structure of the scattering matrix element. These amplitudes are dominated by the exchange of the spin-1 gluon. If this scattering were identical to Rutherford scattering, the angular variable $\chi=(1+|\cos\theta_{\rm cm}|)/(1-|\cos\theta_{\rm cm}|)$ would provide $d\sigma/d\chi=$constant. The data shown in Fig. 6 for dijet production show that the spin-1 exchange process is dominant, with clearly visible differences required by QCD, including the varying α_S. These data also demonstrate the *absence* of further substructure (of the partons) to distance scales approaching 10^{-19} m.

Many other measurements test the correctness of QCD in the perturbative regime. Production of photons and W and Z bosons occurring in hadron collisions are well described by QCD. Production of heavy quark pairs, such as $t\bar{t}$, is not only sensitive to perturbative processes, but also reflects additional effects due to multiple-gluon radiation from the scattering quarks. Within the limited statistics of current data samples, the top quark production cross section is also in good agreement with QCD.

5. Nonperturbative QCD

Many physicists believe that QCD is a theory "solved in principle." The basic validity of QCD at large Q^2, where the coupling is small, has been verified in many experimental studies, but the large coupling at low-Q^2 makes calculation exceedingly difficult. This low-Q^2 region of QCD is relevant to the wealth of experimental data on the static properties of nucleons, most hadronic

interactions, hadronic weak decays, nucleon and nucleus structure, proton and neutron spin structure, and systems of hadronic matter with very high temperature and energy densities. The ability of theory to predict such phenomena has yet to match the experimental progress.

Several techniques for dealing with nonperturbative QCD have been developed. The most successful address processes in which some energy or mass in the problem is large. An example is the confrontation of data on the rates of mesons containing heavy quarks (c or b) decaying into lighter hadrons, where the heavy quark can be treated nonrelativistically and its contribution to the matrix element is taken from experiment. With this phenomenological input, the ratios of calculated partial decay rates agree well with experiment. Calculations based on evaluation at discrete space-time points on a lattice and extrapolated to zero spacing have also had some success. With computing advances and new calculational algorithms, the lattice calculations are now advanced to the stage of calculating hadronic masses, the strong-coupling constant, and decay widths to within roughly (10–20)% of the experimental values.

The quark and gluon content of protons are consequences of QCD, much as the wave functions of electrons in atoms are consequences of electromagnetism. Such calculations require nonperturbative techniques. Measurements of the small-x proton structure functions at the HERA ep collider show much larger increases in parton density with decreasing x than were extrapolated from larger x measurements. It was also found that a large fraction ($\sim$10%) of such events contained a final-state proton essentially intact after collision. These were called ''rapidity gap'' events because they were characterized by a large interval of polar angle (or rapidity) in which no hadrons were created between the emerging nucleon and the jet. More typical events contain hadrons in this gap due to the exchange of the color charge between the struck quark and the remnant quarks of the proton. Similar phenomena have also been seen in hadron-hadron and photon-hadron scattering processes. Calculations that analytically resum whole categories of higher-order subprocesses have been performed. In such schemes, the agent for the elastic or quasielastic scattering processes is termed the ''Pomeron,'' a concept from the Regge theory of a previous era, now viewed as a colorless conglomerate of colored gluons. These ideas have provided semiquantitative agreement with data coming from the ep collider at DESY and the Tevatron.

B. Establishing the electroweak interaction

1. Neutral currents in neutrino scattering

Though the electroweak theory had been proposed by 1968, it received little experimental attention until early in the next decade, when it was shown that all such gauge theories are renormalizable. The electroweak theory specifically proposed a new neutral-current weak interaction.

For virtually any scattering or decay process in which a photon might be exchanged, the neutral-current interaction required added Feynman diagrams with Z exchange and predicted modifications to known processes at very small levels. However, Z exchange is the only mechanism by which an electrically neutral neutrino can scatter elastically from a quark or from an electron, leaving a neutrino in the final state. The theory predicted a substantial rate for this previously unanticipated ν-induced neutral-current process. The only competitive interactions were the well-known charged-current processes with exchange of a W and a charged final-state lepton.

The neutral-current interactions were first seen at CERN in 1973 with scattering from nuclei at rates about 30% of the charged-current scattering (as well as hints of a purely leptonic neutrino interaction with electrons). The results were initially treated with skepticism, since similar experiments had determined limits close to and even below the observed signal, and other contemporary experiments at higher energy obtained results that were initially ambiguous. By 1974, positive and unambiguous results at FNAL had corroborated the existence of the neutral-current reaction using high-energy ν's. In subsequent FNAL and CERN measurements using $\overline{\nu}$'s as well as ν's, the value of ρ was determined to be near unity, and the value of the weak angle, $\sin^2\theta_w$, was established. With time, the values of these parameters have been measured more and more accurately, at low and high energies, in ν reactions with electrons as well as with quarks. All are consistent with the electroweak theory and with a single value of $\sin^2\theta_w$. Figure 7 shows the characteristics of these charged-current and neutral-current events.

2. Photon and Z interference

The neutral current was found at about the anticipated level in several different neutrino reactions, but further verification of its properties were sought. Though reactions of charged leptons are dominated by photon exchange at accessible fixed-target energies, the parity-violating nature of the small Z-exchange contribution permits very sensitive experimental tests. The vector part of the neutral-current amplitude interferes constructively or destructively with the dominant electromagnetic amplitude. In 1978, the first successful such effort was reported, using the polarized electron beam at SLAC to measure the scattering asymmetry between right-handed and left-handed beam electrons. Asymmetries of about 10^{-4} were observed, using several different energies, implying a single value of $\sin^2\theta_w$, in agreement with neutrino measurements.

High-energy e^+e^- collisions provided another important opportunity to observe $\gamma-Z$ interference. By 1983 several experiments at DESY had observed the electromagnetic-weak interference in processes where the e^- and e^+ annihilate to produce a final-state μ pair or τ pair. The asymmetry grows rapidly above a center-of-mass (c.m.) energy of 30 GeV, then changes sign as

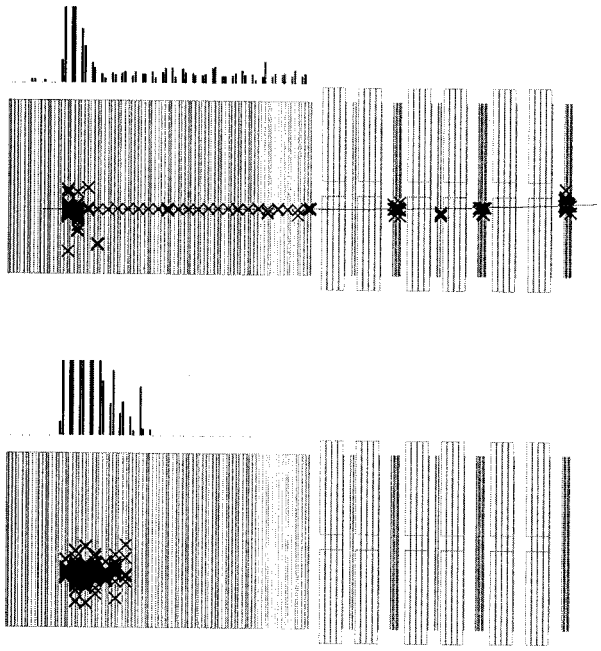

FIG. 7. Displays of events created by ν_μ's in the CCFR experiment at Fermilab. The upper picture is a charged-current interaction, the lower a neutral-current interaction. In each case, the ν enters from the left and interacts after traversing about 1 m of steel. The charged-current event contains a visible energetic μ, which penetrates more than 10 m of steel; the neutral-current event contains an energetic final state ν, which passes through the remainder of the apparatus without trace. Each $(\times)$ records a hit in the sampling planes, and the histogram above the display shows the energy deposition in the scintillator planes interspersed in the steel. The energy near the interaction vertex results from produced hadrons.

the energy crosses the Z resonance. The weak electromagnetic interference is beautifully confirmed in the LEP data, as shown in Fig. 8.

3. Discovery of W and Z

With the corroborations of the electroweak theory with $\rho \sim 1$ and several consistent measurements of the one undetermined parameter, $\sin^2\theta_w$, reliable predictions existed by 1980 for the masses of the vector bosons W and Z. The predicted masses, about 80 and 90 GeV, respectively, were not accessible to e^+e^- colliders or fixed-target experiments, but adequate c.m. energy was possible with existing proton accelerators, so long as the collisions were between two such beams. Unfortunately, none had the two rings required to collide protons with protons.

A concerted effort was mounted at CERN to find the predicted bosons. To save the cost and time of building a second accelerating ring, systems were constructed to produce and accumulate large numbers of antiprotons, gather these and "cool" them into a beam, and then accelerate them in the existing accelerator to collide with a similar beam of protons. In 1983, the W and Z decays were observed with the anticipated masses. Present-day measurements from LEP (Fig. 9) give a

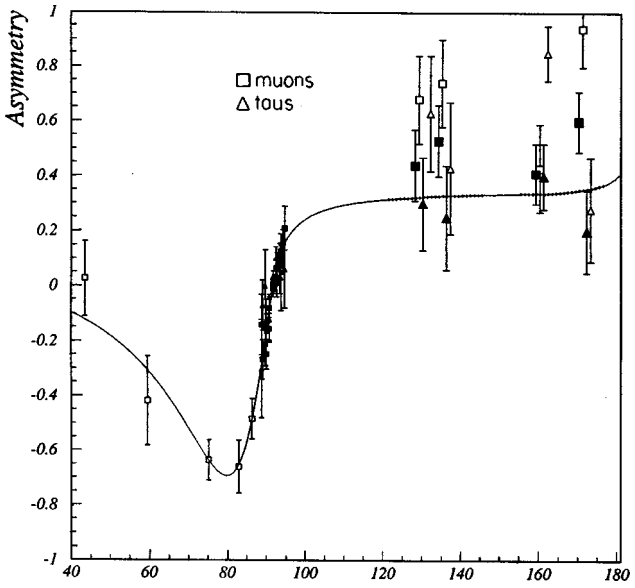

FIG. 8. Forward-backward asymmetry in $e^+e^- \to \mu^+\mu^-$ and $e^+e^- \to \tau^+\tau^-$ as a function of energy from the DELPHI experiment at LEP. The interference of γ and Z contributions gives the asymmetry variation with energy, as indicated by the standard-model curve.

fractional Z mass precision of about 10^{-5} and studies at the FNAL $p\bar{p}$ collider give a fractional W mass precision of about 10^{-3} (Fig. 10).

4. Z properties and precision tests of the electroweak standard model

The LEP and SLAC linear collider experiments have made many precise measurements of the properties of

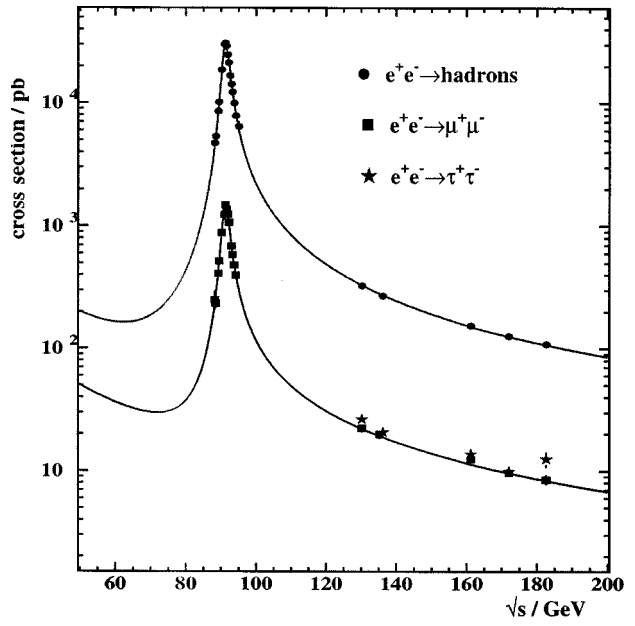

FIG. 9. Dielectron invariant-mass distribution for $ee \to$ hadrons and $ee \to \mu\mu$ from the LEP collider experiments. The prominent Z resonance is clearly apparent.

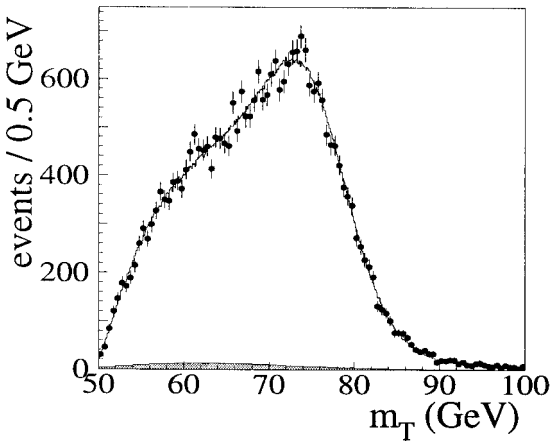

FIG. 10. Transverse mass distribution for $W \to e\nu$ from the DØ experiment. The transverse mass is defined as $M_T = [2E_T^e E_T^\nu (1-\cos\phi^{e\nu})]^{1/2}$ with E_T^e and E_T^ν the transverse energies of electron and neutrino and $\phi^{e\nu}$ the azimuthal angle between them. M_T has its Jacobian edge at the mass of the W boson.

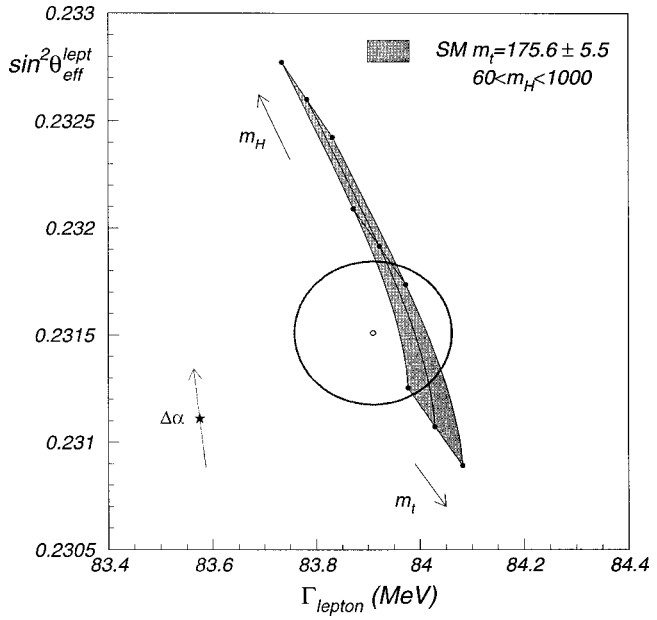

FIG. 11. The allowed region for $\sin^2\theta_w$ vs Γ_{lepton} in the context of the standard model, showing the need for the higher-order electroweak corrections. The region within the ellipse is allowed (at 1 standard deviation) by the many precision measurements at the LEP and SLC ee colliders and the FNAL $p\bar{p}$ collider; the shaded region comes from the measurements of the top mass at FNAL, for a range of possible Higgs masses. The star, well outside the allowed region, gives the expected value in the standard model without the higher-order electroweak corrections.

the Z, refining and testing the electroweak model. The asymmetries due to weak electromagnetic interference discussed above were extended to include all lepton species, c- and b-quark pairs, and light-quark pairs, as well as polarization asymmetries involving τ pairs and initial-state left- or right-handed electrons. From these data, the underlying vector and axial couplings to fermions have been extracted and found to be in excellent agreement with the standard model and with lepton universality. The fundamental weak mixing parameter, $\sin^2\theta_w$, has been determined from these and other inputs to be 0.23152 ± 0.00023.

The total width of the Z is determined to be 2.4948 ± 0.0025 GeV; the invisible decay contributions to this total width allow the number of light ($m_\nu < m_Z/2$) neutrino generations to be measured: $N_\nu = 2.993 \pm 0.011$, confirming another aspect of the standard model. The partial widths for the Z were measured, again testing the standard model to the few-percent level and restricting possible additional non–standard-model particle contributions to the quantum loop corrections. The electroweak and QCD higher-order corrections modify the expectations for all observables. Figure 11 shows the allowed values in the $\sin^2\theta_w$ vs Γ_{lepton} plane under the assumption that the standard model is valid. Even accounting for uncertainties in the Higgs boson mass, it is clear that the higher-order electroweak corrections are required.

Taken together, the body of electroweak observables tests the overall consistency of the standard model. Extensions of the standard model would result in modification of observables at quantum loop level; dominant non-standard-model effects should modify the vacuum polarization terms and may be parametrized in terms of weak-isospin-conserving (S) and weak-isospin-breaking (T) couplings. S and T may be chosen to be zero for specific top quark and Higgs mass values in the minimal standard model; Fig. 12 shows the constraints afforded by several precision measurements and indicates the level to which extensions to the standard model are ruled out.

5. The top quark

The top quark was expected even before measurements in e^+e^- scattering unambiguously determined the b quark to be the $I_3 = -\frac{1}{2}$ member of an isospin doublet. In 1995, the two FNAL $p\bar{p}$ collider experiments reported the first observations of the top. Though expected as the last fermion in the standard model, its mass of about 175 GeV is startlingly large compared to its companion b, at about 4.5 GeV, and to all other fermion masses. The t decays nearly always into a W and a b, with final states governed by the subsequent decay of the W. The large top quark mass gives it the largest fermionic coupling to the Higgs sector. Since its mass is of order the Higgs vacuum expectation value $\langle|\phi|\rangle$, it is possible that the top plays a unique role in electroweak symmetry breaking. The top quark mass is now measured with a precision of about 3%. Together with other precision electroweak determinations, the mass gives useful standard-model constraints on the unknown Higgs boson mass, as shown in Fig. 13. At present, measurements require a standard-model Higgs boson mass less than 420 GeV at 95% confidence level. Such constraints place the Higgs boson, if it exists, within the range of anticipated experiments.

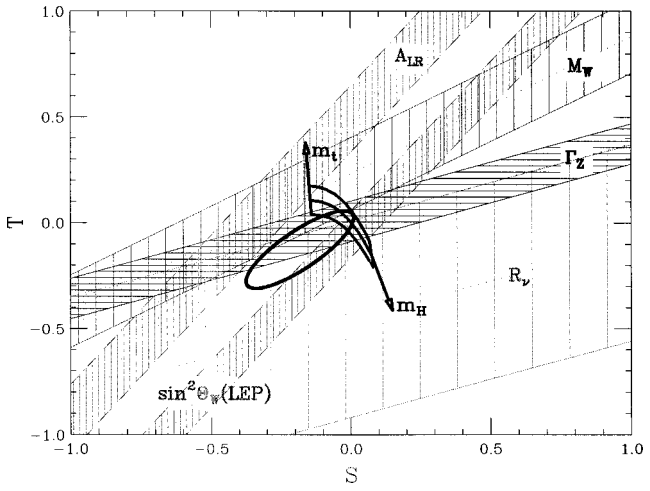

FIG. 12. Several precise electroweak measurements in terms of the S and T variables which characterize the consistency of observables with the standard model. The bands shown from the experimental measurements of A_{LR} (SLC), Γ_Z (LEP), $\sin^2\theta_w$ (LEP), M_W (FNAL and CERN), and R_ν (ν deep-inelastic scattering experiments at CERN and FNAL) indicate the allowed regions in S, T space. The half-chevron region centered on $S=T=0$ gives the prediction for top mass = 175.5±5.5 GeV and Higgs mass between 70 and 1000 GeV, providing the standard model is correct. A fit to all electroweak data yields the 68% confidence region bounded by the ellipse and shows the consistency of the data and the agreement with the minimal standard-model theory.

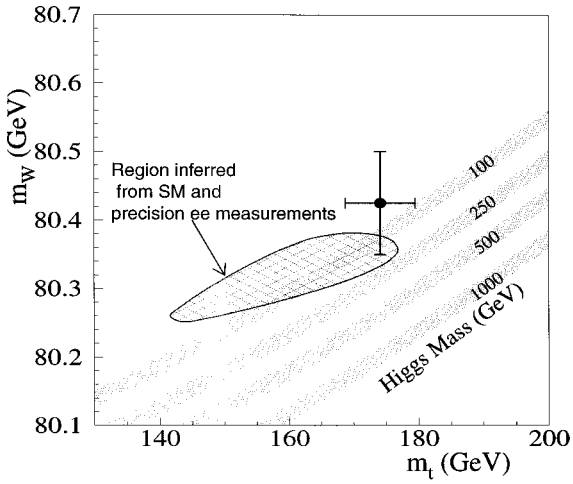

FIG. 13. W boson mass vs top quark mass. The data point is the average of FNAL data for the top quark mass and FNAL and CERN data for the W boson mass. The shaded bands give the expected values for specific conventional Higgs boson mass values in the context of the minimal standard model. The cross-hatched region shows the predictions for m_W and m_{top}, at 68% confidence level, from precision electroweak measurements of Z boson properties.

6. Trilinear gauge couplings

The gauge symmetry of the electroweak standard model exactly specifies the couplings of the W, Z, and γ bosons to each other. These gauge couplings may be probed through the production of boson pairs: WW, $W\gamma$, WZ, $Z\gamma$, and ZZ. The standard model specifies precisely the interference terms for all these processes. The diboson production reactions have been observed in FNAL collider experiments and the WW production has been seen at LEP. Limits have been placed on possible anomalous couplings beyond the standard model. For $WW\gamma$, the experiments have shown that the full electroweak gauge structure of the standard model is necessary, as shown in Fig. 14, and constrain the anomalous magnetic dipole and electric quadrupole moments of the W.

7. Quark mixing matrix

The generalization of the rotation of the down-strange weak-interaction eigenstates from the strong-interaction basis indicated in Eq. (2) to the case of three generations gives a 3×3 unitary transformation matrix $\mathbf{V}$, whose elements are the mixing amplitudes among the d, s, and b quarks. Four parameters—three real numbers (e.g., Euler angles) and one phase—are needed to specify this matrix. The real elements of this Cabibbo-Kobayashi-Maskawa (CKM) matrix are determined from various experimental studies of weak flavor-changing interactions and decays. The decay rates of c and b quarks depend on the CKM elements connecting the second and third generation. These have been extensively explored in e^+e^- and hadronic collisions which copiously produce B and charmed mesons at Cornell, DESY, and FNAL. The pattern that emerges shows a hierarchy in which the mixing between first and second generation is of order the Cabibbo angle, $\lambda=\sin\theta_c$, those between the second and third generation are of order λ^2, and those between first and third generation are of order λ^3.

A nonzero CKM phase would provide CP-violating effects such as the decay $K_L^0\to\pi\pi$, as well as different decay rates for B^0 and $\overline{B}^0$ into CP-eigenstate final states. CP violation has only been observed to date in

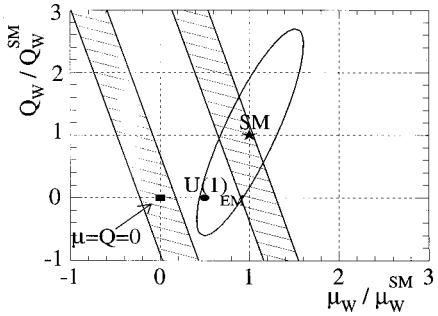

FIG. 14. The W boson electric quadrupole moment vs magnetic dipole moment from $W\gamma$ production relative to their standard-model values. The ellipse shows the 95% confidence level limit from the DØ experiment with both Q and μ allowed to vary. Limits from $b\to s\gamma$ from CLEO at Cornell and ALEPH at LEP are shown as the hatched bands. The star shows the moments if the standard-model couplings are correct; the filled circle labeled $\mathrm{U(1)_{EM}}$ corresponds to a standard-model SU(2) coupling of zero.

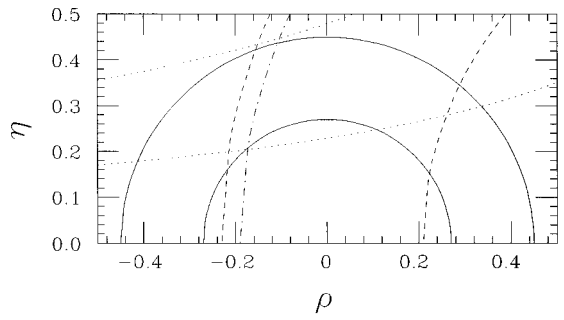

FIG. 15. Experimentally allowed regions in the $\rho\eta$ plane from experiments. The region between the solid semicircles is from the ratio of b quark decays into u or c quarks. The CP-violating amplitudes from K_L^0 decays give the band between the dotted hyperbolae. The region between the dashed semicircles is allowed by measurements of B^0-$\overline{B}^0$ mixing. The constraint imposed from current limits on B_s^0-$\overline{B}_s^0$ mixing is to the right of the dot-dashed semicircle. Current experiments thus are consistent, and favor nonzero values of the CP-violating parameter η.

the neutral-K decays, where it is consistent with (though not requiring) the description embodied in the CKM matrix. Well-defined predictions of the CKM phase for a variety of B-decay asymmetries will be tested in experiments at SLAC, KEK in Japan, Cornell, DESY, and FNAL in the coming few years. The unitarity relations $\mathbf{V}_{ij}^{\dagger}\mathbf{V}_{jk}=\delta_{ik}$ impose constraints on the observables that must be satisfied if CP violation is indeed embedded in the CKM matrix and if there are but three quark generations. Figure 15 shows the current status of the constraints on the real and imaginary parts (ρ,η) of the complex factor necessary if the origins of CP violation are inherent to the CKM matrix.

VII. UNRESOLVED ISSUES: BEYOND THE STANDARD MODEL

While the standard model has proven highly successful in correlating vast amounts of data, a major aspect of it is as yet untested, namely, the origin of electroweak symmetry breaking. The Higgs mechanism described in Sec. IV is just the simplest ansatz that is compatible with observation. It predicts the existence of a scalar particle, but not its mass; current LEP data provide a lower limit: $m_H>80$ GeV. The Higgs mass is determined by its coupling constant λ [cf. Eq. (3)] and its vacuum value v: $m_H\approx\lambda\times 348$ GeV. A Higgs mass of a TeV or more would imply strong coupling of longitudinally polarized W and Z bosons that are the remnants of the "eaten" Goldstone boson partners of the physical Higgs particle. It can be shown quite generally that if there is no Higgs particle with a mass less than about a TeV, strong W,Z scattering will occur at TeV c.m. energies; the observation of this scattering requires multi-TeV proton-proton c.m. energies, as will be achieved at the LHC.

However, the introduction of an elementary scalar field in quantum field theory is highly problematic. Its mass is subject to large quantum corrections that make it difficult to understand how it can be as small as a TeV or less in the presence of large scales in nature like the Planck scale of 10^{19} GeV or possibly a scale of coupling-constant unification at 10^{16} GeV. Moreover, a strongly interacting scalar field theory is not self-consistent as a fundamental theory: the coupling constant grows with energy and therefore any finite coupling at high energy implies a weakly coupled theory at low energy. There is therefore strong reason to believe that the simple Higgs mechanism described in Sec. IV is incorrect or incomplete and that electroweak symmetry breaking must be associated with fundamentally new physics. Several possibilities for addressing these problems have been suggested; their common thread is the implication that the standard model is an excellent low-energy approximation to a more fundamental theory and that clues to this theory should appear at LHC energies or below.

For example, if quarks and leptons are composites of yet more fundamental entities, the standard model is a good approximation to nature only at energies small compared with the inverse radius of compositeness Λ. The observed scale of electroweak symmetry breaking, $v\sim\frac{1}{4}$ TeV, might emerge naturally in connection with the compositeness scale. A signature of compositeness would be deviations from standard-model predictions for high-energy scattering of quarks and leptons. Observed consistency (e.g., Fig. 6) with the standard model provides limits on Λ that are considerably higher than the scale v of electroweak symmetry breaking.

Another approach seeks only to eliminate the troublesome scalars as fundamental fields. Indeed, the spontaneous breaking of chiral symmetry by a quark-antiquark condensate in QCD also contributes to electroweak symmetry breaking. If this were its only source, the W,Z masses would be determined by the 100-MeV scale at which QCD is strongly coupled: $m_W=\cos\theta_w m_Z\approx 30$ MeV. To explain the much larger observed masses, one postulates a new gauge interaction, called technicolor, that is strongly coupled at the scale $v\sim\frac{1}{4}$ TeV. At this scale fermions with technicolor charge condense, spontaneously breaking both a chiral symmetry and the electroweak gauge symmetry. The longitudinally polarized components of the massive W and Z are composite pseudoscalars that are Goldstone bosons of the broken chiral symmetry, analogous to the pions of QCD. This is a concrete realization of a scenario with no light scalar particle, but with strong W,Z couplings in the TeV regime, predicting a wealth of new composite particles with TeV masses. However, it has proven difficult to construct explicit models that are consistent with all data, especially the increasingly precise measurements that probe electroweak quantum corrections to W and Z self-energies; these data (Figs. 12 and 13) appear to favor an elementary scalar less massive than a few hundred GeV.

The quantum instability of elementary scalar masses can be overcome by extending the symmetry of the

theory to one that relates bosons to fermions, known as supersymmetry. Since quantum corrections from fermions and bosons have opposite signs, many of them cancel in a supersymmetric theory, and scalar masses are no more unstable than fermion masses, whose smallness can be understood in terms of approximate chiral symmetries. This requires doubling the number of spin degrees of freedom for matter and gauge particles: for every fermion f there is a complex scalar partner $\tilde{f}$ with the same internal quantum numbers, and for every gauge boson v there is a spin-$\frac{1}{2}$ partner $\tilde{v}$. In addition, the cancellation of quantum gauge anomalies and the generation of masses for all charged fermions requires at least two distinct Higgs doublets with their fermion superpartners. Mass limits on matter and gauge superpartners ($m_{\tilde{\gamma},\tilde{W}}>50$ GeV, $m_{\tilde{q},\tilde{g}}>200$ GeV) imply that supersymmetry is broken in nature. However, if fermion-boson superpartner mass splittings are less than about a TeV, quantum corrections to the Higgs mass will be suppressed to the same level. For this scenario to provide a viable explanation of the electroweak symmetry-breaking scale, at least some superpartners must be light enough to be observed at the LHC.

Another untested aspect of the standard model is the origin of CP violation, conventionally introduced through complex Yukawa couplings of fermions to Higgs particles, resulting in complex parameters in the CKM matrix. This ansatz is sufficient to explain the observed CP violation in K decay, is consistent with limits on CP violation in other processes, and predicts observable CP-violating effects in B decay. Planned experiments at new and upgraded facilities capable of producing tens of millions of B mesons will determine whether this model correctly describes CP violation, at least at relatively low energy. A hint that some other source of CP violation may be needed, perhaps manifest only at higher energies, comes from the observed predominance of matter over antimatter in the universe.

While in the minimal formulation of the standard model neutrinos are massless and exist only in left-handed states, there have been persistent indirect indications for both neutrino masses and mixing of neutrino flavors. Nonzero neutrino mass and lepton flavor violation would produce spontaneous oscillation of neutrinos from one flavor to another in a manner similar to the strangeness oscillations of neutral-K mesons. Solar neutrinos of energies between 0.1 and 10 MeV have been observed to arrive at the earth at a rate significantly below predictions from solar models. A possible interpretation is the oscillation of ν_e's from the solar nuclear reactions to some other species, not observable as charged-current interactions in detectors due to energy conservation. Model calculations indicate that both solar-matter-enhanced neutrino mixing and vacuum oscillations over the sun-earth transit distance are viable solutions. A deficit of ν_μ relative to ν_e from the decay products of mesons produced by cosmic-ray interactions in the atmosphere has been seen in several experiments. Recent data from the Japan-U.S. SuperKamiokande experiment, a large water Cerenkov detector located in Japan, corroborate this anomaly. Furthermore, their observed ν_μ and ν_e neutrino interaction rates plotted against the relativistic distance of neutrino transit (Fig. 16) provide strong evidence for oscillation of ν_μ into ν_τ—or into an unseen "sterile" neutrino. An experimental anomaly observed at Los Alamos involves an observation of ν_e interactions from a beam of ν_μ. These indications of neutrino oscillations are spurring efforts worldwide to resolve the patterns of flavor oscillations of massive neutrinos.

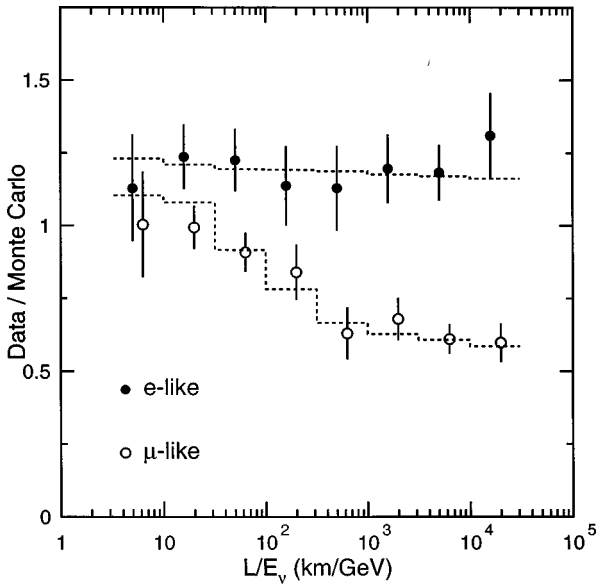

FIG. 16. The ratio of the number of ν_e and ν_μ interactions in the SuperKamiokande detector to the Monte Carlo expectations for each, as a function of L/E_ν, where L is the distance of travel from neutrino production in the earth's atmosphere and E_ν is the neutrino energy. Neutrinos produced on the far side of the earth and going upwards in the detector contribute at the largest L/E_ν. The Monte Carlo curves are computed for the best-fit difference in mass squared between oscillating neutrinos of 2.2×10^{-3} eV^2 and maximal mixing.

The origins of electroweak symmetry breaking and of CP violation, as well as the issue of the neutrino mass, are unfinished aspects of the standard model. However, the very structure of the standard model raises many further questions, strongly indicating that this model provides an incomplete description of the elementary structure of nature.

The standard model is characterized by a large number of parameters. As noted above, three of these—the gauge coupling constants—approximately unify at a scale of about 10^{16} GeV. In fact, when the coupling evolution is calculated using only the content of the standard model, unification is not precisely achieved at a single point: an exact realization of coupling unification requires new particles beyond those in the standard model spectrum. It is tantalizing that exact unification can be achieved with the particle content of the minimal supersymmetric extension of the standard model if superpartner masses lie in a range between 100 GeV and 10 TeV (Fig. 17).

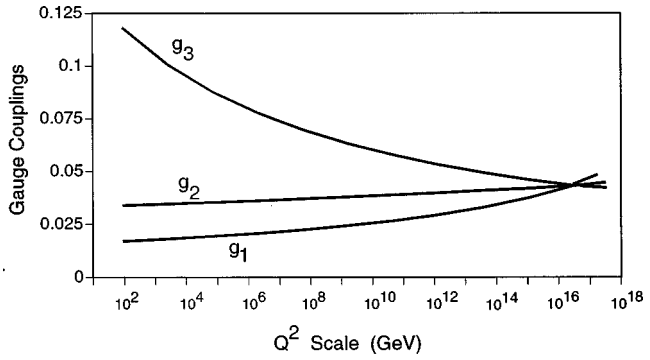

FIG. 17. Gauge couplings g_1, g_2, g_3 as a function of Q^2 in the context of the minimal supersymmetric model, showing unification around 10^{16} GeV.

Coupling unification, if true, provides compelling evidence that, above the scale of unification, physics is described by a more fundamental theory incorporating the standard-model interactions in a fully unified way. One possibility, grand unified theory, invokes a larger gauge group, characterized by a single coupling constant, which is broken to the standard-model gauge group by a Higgs vacuum value, $v \sim 10^{16}$ GeV. Couplings differ at low energies because some particles acquire large masses from this Higgs field; symmetry is restored at energy scales above 10^{16} GeV, where these masses are unimportant. Another possibility is that a completely different theory emerges above the scale of unification, such as a superstring theory in ten-dimensional spacetime—perhaps itself an approximation to a yet more fundamental theory in eleven dimensions (see the following article). In string-derived models, coupling unification near the string scale is due to the fact that all gauge coupling constants are determined by the vacuum value of a single scalar field.

Most of the remaining parameters of the standard model, namely, the fermion masses and the elements of the CKM matrix (including a CP-violating phase), are governed by Yukawa couplings of fermions to the Higgs fields. The observed hierarchies among quark fermion masses and mixing parameters are strongly suggestive that new physics must be at play here as well. If there are no right-handed neutrinos, the standard model, with its minimal Higgs content, naturally explains the absence, or very strong suppression, of neutrino masses. However, many extensions of the standard model, including Grand Unified Theory and string-derived models, require right-handed neutrinos, in which case additional new physics is needed to account for the extreme smallness of neutrino masses.

Many models have been proposed in attempts to understand the observed patterns of fermion masses and mixing. These include extended gauge or global symmetries, some in the context of Grand Unified Theory or string theory, as well as the possibility of quark and lepton compositeness. Unlike the issues of electroweak symmetry breaking and CP violation, there is no well-defined energy scale or set of experiments that is certain to provide positive clues, but these questions can be attacked on a variety of fronts, including precision measurements of the CKM matrix elements, searches for flavor-changing transitions that are forbidden in the standard model, and high-energy searches for new particles such as new gauge bosons or excited states of quarks and leptons.

The standard model has another parameter, θ, that governs the strength of CP violation induced by nonperturbative effects in QCD. The experimental limit on the neutron electric dipole moment imposes the constraint $\theta < 10^{-9}$, again suggestive of an additional symmetry that is not manifest in the standard model. Many other questions remain unresolved; some have profound implications for cosmology, discussed in Sec. V. Is the left/right asymmetry of the electroweak interaction a fundamental property of nature, or is mirror symmetry restored at high energy? Is the proton stable? Grand Unified Theory extensions of the standard model generally predict proton decay at some level, mediated by bosons that carry both quark and lepton numbers. Why are there three families of matter? Some suggested answers invoke extended symmetries; others conjecture fermion compositeness; in string theory the particle spectrum of the low-energy theory is determined by the topology of the compact manifold of additional spatial dimensions. Why is the cosmological constant so tiny, when, in the context of quantum field theory, one would expect its scale to be governed by other scales in the theory, such as the electroweak symmetry-breaking scale of a TeV, or the Planck scale of 10^{19} GeV? The standard model is incomplete in that it does not incorporate gravity. Superstrings or membranes, the only candidates at present for a quantum theory of gravity, embed the standard model in a larger theory whose full content cannot be predicted at present, but which is expected to include a rich spectrum of new particles at higher energies.

Future experiments can severely constrain possible extensions of the standard model, and the discovery of unanticipated new phenomena may provide a useful window into a more fundamental description of nature.

Thousands of original papers have contributed to the evolution of the standard model. We apologize for omitting references to these, and for the necessarily incomplete coverage of many incisive results. We list some recent reviews (Quigg, 1983; Weinberg, 1993; Darriulat, 1995; Veneziano, 1997; Dawson, 1998), which give an entry into this illuminating and impressive literature.

REFERENCES

Darriulat, P., in *Proceedings of the XXVII International Conference on High Energy Physics*, Glasgow, Scotland, 1995, edited by P. J. Bussey and I. G. Knowles (Institute of Physics, Bristol), p. 367.

Dawson, S., 1998, in *Proceedings of the 1996 Annual Divisional Meeting of the Division of Particles and Fields*, Minneapolis, Minnesota, 1996, in press.

Quigg, C., 1983, *Gauge Theories of the Strong, Weak, and Electromagnetic Interactions* (Benjamin/Cummings, New York).

Veneziano, G., 1996, in *Proceedings of the XXVII International Conference on High Energy Physics*, Warsaw, Poland, 1996, edited by Z. Ajduk and A. K. Wroblewski (World Scientific, Singapore), p. 449.

Weinberg, S., 1993, in *Proceeding of the XXVI International Conference on High Energy Physics*, Dallas, Texas 1992, AIP Conf. Proc. No. 272, edited by J. R. Sanford (AIP, New York), p. 346.